

# Preparation and characterization of chitosan-poly (vinyl alcohol)/polyvinylidene fluoride hollow fiber composite membranes for pervaporation dehydration of isopropanol

Jing Wang, Wenying Zhang, Weixing Li<sup>†</sup>, and Weihong Xing

State Key Laboratory of Materials-Oriented Chemical Engineering, College of Chemistry and Chemical Engineering,  
Nanjing Tech University, Nanjing 210009, China

(Received 17 March 2014 • accepted 7 November 2014)

**Abstract**—A new hollow fiber composite membrane of chitosan-poly (vinyl alcohol)/polyvinylidene fluoride (CS-PVA/PVDF) was prepared by casting the solution of CS and PVA on PVDF hollow fiber support for pervaporation dehydration of isopropanol. The composite membranes were crosslinked with glutaraldehyde (GA) and sulfuric acid. The microstructure and physicochemical properties of the membranes were characterized by scanning electron microscope (SEM), attenuated total reflection-Fourier transform infrared spectroscopy (ATR-FTIR), thermogravimetry (TG) and contact angle measurements. Results from SEM images showed that dense separation layers were successfully coated onto the supports, and the ATR-FTIR results showed that GA had crosslinked the composite membranes. Results of TG and contact angle showed the thermostability of membranes increased and the hydrophilicity decreased after blending CS and PVA. The swelling degree of composite membranes increased with increasing CS content and water content. Effects of the content of CS and GA in solution on membrane separation performance were investigated. The pervaporation experiments for dehydration of isopropanol showed that the membrane with 60 wt% CS and 0.1 wt% GA had a good separation performance. The permeate flux was 306 g/(m<sup>2</sup>·h) and the separation factor was 2140 for the feed solution containing 90% isopropanol at 60 °C. When the water content increased from 3 wt% to 15 wt%, the permeate flux increased from 207 g/(m<sup>2</sup>·h) to 346 g/(m<sup>2</sup>·h) while the separation factor decreased from 2406 to 1876. The separation factor and permeation flux increased with feed temperature.

Keywords: Pervaporation, Chitosan, Polyvinyl Alcohol, Isopropanol

## INTRODUCTION

Pervaporation (PV) is a new type of membrane separation technology with a wide range of uses such as dehydration of solvents and separation of organic mixtures [1]. In the PV process, separation is based on the transport of the components through the membrane, which is determined by the solubility and diffusivity of the components to be separated. Compared with distillation, it has many advantages in separation of azeotropic mixtures and close boiling-point mixtures [2]. As an important chemical product, isopropanol (IPA) is mainly used in pharmaceutical, plastic, coating and variety of cosmetics. It is well known that water and IPA can form azeotrope with the IPA content of 87.8 wt% at 80.3 °C, which causes difficulty in its recovery through the distillation process. Therefore, dehydration of IPA coupled by PV with a suitable membrane material is focused on. Sajjan et al. [3] developed novel grafted hybrid PVA membranes for pervaporation dehydration of IPA, and the membrane exhibited the separation selectivity of 1570 with a flux of 19.2 g/(m<sup>2</sup>·h). Svang-Ariyaskul et al. [4] prepared blended CS-PVA membranes that showed good performance for pervaporation dehydration of IPA. Suhas et al. developed mixed matrix mem-

branes of poly(vinyl alcohol) loaded with zeolite particles [5] and graphene-loaded sodium alginate nanocomposite membranes [6] for dehydration of IPA. The improvement in membrane performance was attributed to favorable interaction between zeolite particles and graphene with the polymer matrix separately. Adoor et al. [7] prepared polymeric nanocomposite membranes containing phosphotungstic acid for pervaporation dehydration of IPA, and the NaAlg membrane containing 10 wt% modified PTA showed the highest PV performance.

Chitosan (CS) contains both active amino groups and hydroxyl groups that can form hydrogen bonds with water. Because of its good film-forming property, high mechanical strength, excellent chemical-resistant and moderate price, CS is widely used in membrane preparation. To enhance the stability and improve the separation performance of CS membranes, modification methods such as blending and cross-linking have been applied by many researchers [8-10]. Poly(vinyl alcohol) (PVA) is one of the most important polymers commonly blended with CS to prepare membrane due to its superior hydrophilic property and chemical stability. Hyder et al. [11] studied the pervaporation performance of CS-PVA blending membranes for dehydration of ethylene glycol. Rao et al. [12] prepared CS and PVA membranes for the dehydration of IPA and tetrahydrofuran through pervaporation, which showed good performance and mechanical strength. To reduce the swelling of blended membranes, glutaraldehyde (GA) is used as an effective crosslinker which

<sup>†</sup>To whom correspondence should be addressed.

E-mail: wxli@njtech.edu.cn

Copyright by The Korean Institute of Chemical Engineers.

**Table 1. Abbreviations of different comparison of membranes**

Content (wt%) \ Membranes	M0	M1	M2	M3	M4	M2-1	M2-2
CS	100	75	60	33.3	0	60	60
PVA	0	25	40	66.7	100	40	40
GA	0.10	0.10	0.10	0.10	0.10	0.05	0.15

can combine CS with PVA through nucleophilic addition reaction. These improved membranes showed great performance for dehydration of organic mixtures. In recent years, the development of nanocomposite membranes of polymers such as sodium alginate, poly(vinyl alcohol) and poly(vinyl pyrrolidone) incorporated with varying nanoparticles such as phosphomolybdic acid, preysler type heteropolyacid, phosphotungstic acid and zeolite particles have also attracted much attention. In these papers, the authors published and analyzed the PV data using sorption-diffusion principles [13-16].

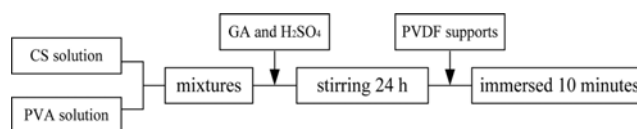
To increase the loading area of membranes, hollow fiber is widely used as the substrate of membranes. In the past few years, the composite membranes that contain a thin and dense separation layer on hollow fiber support have been focused on. Liu et al. [17] developed dual-layers P84/PES hollow fibers with p-xylenediamine cross-linking for pervaporation dehydration of IPA that showed high separation factor 953 with the permeate flux 454 g/(m<sup>2</sup>·h). Yuan et al. [18] prepared the PVA/PAN composite membrane by dip-coating method for dehydration of ethyl acetate/water solution and the separation factor was 7270. Poly(vinylidene fluoride) (PVDF) is one of the most extensively applicable membrane materials commonly used as a porous substrate for its outstanding antioxidation, superior thermal and excellent chemical stability [19]. PVDF hollow fiber ultrafiltration membrane was alternative membrane materials for separation of organic mixtures and water treatment industry [20-22]. Zhao et al. [20] prepared the PVDF hollow fiber membrane modified with CS that provided an excellent performance in the water-protein liquid filtration. Sukitpaneenit et al. [21] developed PVDF asymmetric hollow fiber membranes, which demonstrated remarkable high fluxes of 3,500-8,800 g/(m<sup>2</sup>·h) and reasonable ethanol-water separation factors of 5-8.

However, the research on PVDF hollow fiber ultrafiltration membrane as substrate of pervaporation membranes for dehydration of IPA has been seldom reported. In this work, we prepared CS-PVA/PVDF hollow fiber membrane crosslinked by GA and sulfuric acid. Effects of the ratio of CS:PVA in casting solutions and the concentration of GA on membrane separation performance were investigated. Meanwhile, the swelling behaviors of composite membranes were discussed. The pervaporation performance of the composite membrane was studied by the dehydration of IPA/H<sub>2</sub>O mixtures.

## EXPERIMENTAL

### 1. Materials

The PVDF hollow fiber membrane supports were prepared by our research team. CS (80 wt% N-deacetylation degree) and PVA (the average degree of polymerization 1750) were obtained from Sin-

**Fig. 1. Schematic diagram of preparation process of the CS-PVA/PVDF membranes.**

opharm Chemical Reagent Co., Ltd. Acetic acid (purity 99.5 wt%) was purchased from Shanghai Shenbo Chemical Reagent Co., Ltd. All other chemicals including isopropanol, glutaraldehyde and sulfuric acid were supplied by Sinopharm Chemical Reagent Co., Ltd. Deionized water was produced by a Milli-Q system (Millipore, US).

### 2. Membrane Preparation

A 1 wt% CS solution was prepared by dissolving CS in 2 wt% aqueous acetic acid solution with stirring for 6 h at 25 °C. PVA was dissolved in deionized water at 100 °C to form a homogeneous solution of 5 wt%. Both solutions were mixed with different CS-PVA ratios (Table 1). Then, different amounts of glutaraldehyde and quantitative of sulfuric acid were added into the mixtures used as cross-linking agent and catalyst. The mixtures were stirred for 24 h to make the solution completely homogeneous. Finally, the PVDF hollow fiber ultrafiltration membrane was immersed in the prepared solutions for 10 minutes, then taken out and fully dried at ambient temperature. Fig. 1 is a schematic diagram of the preparation process of the CS-PVA/PVDF membranes.

To measure the thermostability and hydrophilicity of composite membranes, the casting solutions were poured onto glass plate and dried at ambient temperature. Then, the dried flat membranes were measured.

### 3. Membrane Characterization

The surface, cross-section morphologies and the thickness of different composite membranes were observed by field-emission scanning electron microscopy (S-4800, Hitachi, Japan). All samples were immersed and freeze-fractured in liquid nitrogen and sputtered with gold before analysis. To characterize the difference of chemical groups, attenuated total reflection-Fourier transform infrared spectroscopy (ATR-FTIR) was used. The FTIR spectra of flat-sheet active separation layers were scanned with an FTIR spectrometer (AVATAR 360, Thermo Nicolet, USA). Thermogravimetric analysis (TG) was conducted under nitrogen atmosphere at a heating rate of 10 °C/min by thermoanalyzer (Sta 449 F3, Netzsch, Germany) in the temperature range 30-700 °C, and 10-15 mg of sample was used for each experiment. The water contact angles of flat-sheet active separation layers were measured by a contact angle meter (DSA100, Kruss, Germany) with a water drop deposited onto the surface kept in 30 seconds. All the contact angle experi-

ments were repeated three times and the results were averaged.

#### 4. Swelling Experiments

The swelling experiments of all membranes were investigated. First, the mass of dry membrane was weighed as  $W_d$ . Then, the sample was immersed in different concentration isopropanol solutions for 24 h to ensure swelling to reach equilibrium at room temperature. The swollen membrane was taken out carefully and the surface solution was wiped off with tissue paper as quickly as possible. The mass of the swollen membrane was measured as  $W_s$ . The swelling degree of the membrane was calculated by Eq. (1):

$$\text{Swelling degree (\%)} = (W_s - W_d) / W_d \times 100\% \quad (1)$$

where  $W_d$  and  $W_s$  are the weights of the dry and swollen membranes, respectively. Every experiment was repeated three times and the average result was used.

#### 5. Pervaporation Experiments

The membrane module consisted of six fibers whose bottom was sealed using epoxy resin with effective area  $0.0016 \text{ m}^2$ ; it was immersed in the feed solution for 1 h to make the membranes to reach a steady state before starting PV experiments. A vacuum pump placed in the downstream was normally maintained at about 200 Pa and monitored by a digital vacuum gauge. The permeate vapor was collected by two liquid nitrogen traps in turn. The permeate flux ( $J$ ,  $\text{g}/(\text{m}^2 \cdot \text{h})$ ) was defined as follows:

$$J = \frac{M}{A \times t} \quad (2)$$

where  $M$  is the total weight of permeate over a certain time interval  $t$ , and  $A$  is the effective membrane area.

The feed and permeate composition of mixtures were determined by gas chromatograph (GC-2014, Shimadzu, Japan) equipped with a thermal conductivity detector (TCD). The column packed with PORAPAK® Q (mesh 50-80) was 2 m in length and helium (99.9999%) was used as the carrier gas. The injector and detector temperatures were both  $200^\circ\text{C}$  and the column temperature was  $180^\circ\text{C}$ . The bridge current was 110 mA and the sample size for GC was  $1 \mu\text{L}$ . The separation factor ( $\alpha$ ) was defined by:

$$\alpha = \frac{(Y_W/Y_I)_{\text{permeate}}}{(X_W/X_I)_{\text{feed}}} \quad (3)$$

where  $Y_W$ ,  $Y_I$ ,  $X_W$  and  $X_I$  are the weight fractions of water and isopropanol in the permeate and feed solutions, respectively.

## RESULTS AND DISCUSSION

### 1. FTIR Analysis

GA could react with the hydroxyl group ( $-\text{OH}$ ) and the amino group ( $-\text{NH}_2$ ) of CS to form aldehyde acetal and Schiff base, as well as the hydroxyl group ( $-\text{OH}$ ) of PVA in the acidic condition [10]. This crosslinking reaction and interaction inhibit the swelling degree of membrane remarkably because of a formed three-dimensional network between the molecules [23,24].

The FTIR spectra of membranes with different ratio of polymer and GA content are illustrated in Fig. 2. The spectra of all membranes show characteristic peaks at  $3,258 \text{ cm}^{-1}$  assigned to  $-\text{OH}$  and  $-\text{NH}_2$  stretching vibrations. The absorption peaks at  $2,914 \text{ cm}^{-1}$

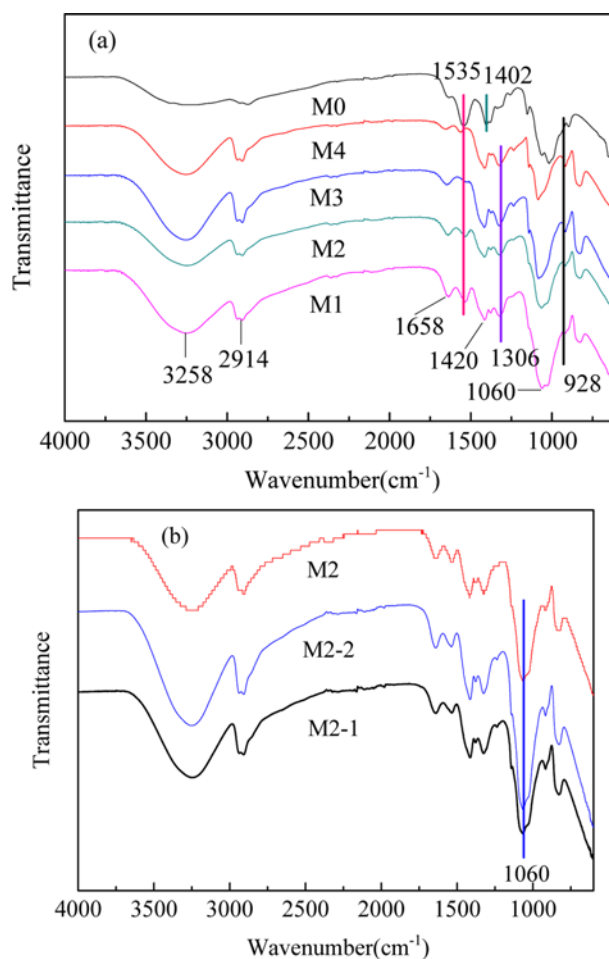


Fig. 2. ATR-FTIR spectra of the membranes: (a) different ratio of polymer membranes, (b) different content of GA membranes.

and  $1,060 \text{ cm}^{-1}$  correspond to saturated stretching of  $-\text{CH}_2$  and  $\text{C}-\text{O}$  groups, respectively [12]. In Fig. 2(a), for the homogeneous CS spectrum, the stretching vibration of  $-\text{NH}_2$  occurs at  $1,402 \text{ cm}^{-1}$  while the rest of the membranes show a little deviation because of the addition of PVA and the peak at  $1,535 \text{ cm}^{-1}$  corresponding to the  $\text{C}\equiv\text{N}$  group which indicates CS has been crosslinked by GA. The  $\text{C}\equiv\text{N}$  characteristic peak intensity gradually is weakened with the decrease of CS content from 75 wt% to 0 wt%. Absorption peaks of  $\text{C}=\text{O}$  can be observed around  $1,658 \text{ cm}^{-1}$ , which suggests the hydroxyl groups react with aldehyde groups. Due to less of  $-\text{OH}$  in CS, a small stretching vibration of  $\text{C}=\text{O}$  could be obtained. Fig. 2(b) shows the  $\text{C}-\text{O}$  absorption band which appears in the peak of  $1,060 \text{ cm}^{-1}$  and it presents a decreasing trend as the crosslinking agent content reduced.

### 2. TG Analysis

The thermal stability of membranes was investigated (Fig. 3). Three main stages of the weight loss related to the processes of thermal dehydration, degradation of side-groups and decomposition of the polymer backbone are presented [25]. In Fig. 3(a), for pure CS membrane M0, a big drop occurs from  $250^\circ\text{C}$  to  $560^\circ\text{C}$  due to the breakdown of the backbone. The weight loss of PVA between  $240^\circ\text{C}$  and  $300^\circ\text{C}$  is around 40% as a result of the degradation of

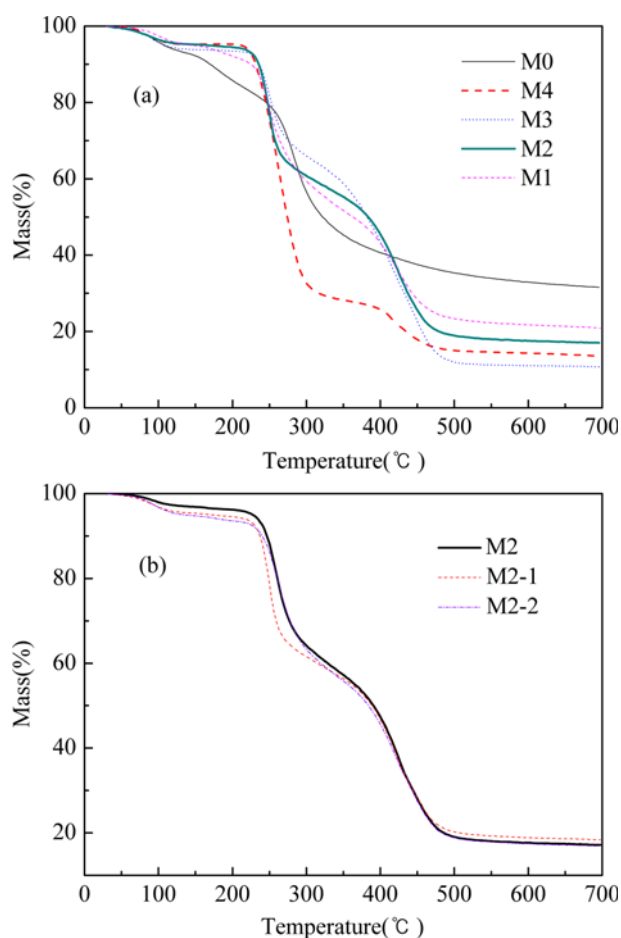


Fig. 3. TG curves of the membranes: (a) different ratio of polymer membranes, (b) different content of GA membranes.

side-groups. After blending the two polymers according to a certain proportion, the thermal stability increases significantly because of the increase of crosslinking degree. Furthermore, the weight loss of M2 at the two and three stages is between M1 and M3 and the stability is better compared with the others. Fig. 3(b) shows the thermal stability of membranes with different content of GA. The result indicates that the trends of membranes weightlessness are essentially the same, so the content of GA has little influence on the TG curves.

### 3. SEM Analysis

Fig. 4 shows the SEM images of hollow fiber membranes. Fig. 4(a) and 4(b) are the external surface and cross-section morphologies of PVDF support. The surface image shows a large number of micropores on the surface of membrane with the pore size of 300 nm. After coating the CS and PVA solution, the surface of membrane M2 was smooth and dense. Meanwhile, the cross-section picture shows that the active separation layer was tightly coated onto the PVDF hollow fiber support membrane. The thickness of the active separation layer was approximately 3.5  $\mu\text{m}$ . By changing the GA content, some sags and crests on the external surface of the prepared membranes appeared in Fig. 4(e) and 4(f).

### 4. Contact Angle Analysis

The results of contact angle experiments are presented in Table

2. The hydrophilicity of the membrane surface is generally quantified by contact angle. From the data in the table, the contact angles of pure CS and PVA membranes are 67.2° and 66.9°, respectively. The water contact angle increases with the increase of CS content in the polymer. The contact angle of pure membrane is smaller than those of the blend membranes, which indicates the crosslinking reaction may decrease the hydrophilicity of the membranes. When the crosslinking agent content increased from 0.05 wt% to 0.15 wt%, the contact angle increased from 74.3° to 85.7°. It suggests that the increase of contact angle resulted from the increasing crosslinking degree of the blend membranes.

### 5. Swelling Behavior

Membrane swelling behavior depends on many factors, including the composition of the polymer, the structure of membrane and the crosslinking density. However, swelling properties can affect the separation factor and permeation flux of the membranes in PV experiments. In Fig. 5, the swelling degree of the membrane increases with the increase of CS content. On one hand, the hydration of CS makes it have large amounts of ammonium salt groups which are positive charges, and so negative ions ( $\text{OH}^-$ ) are attracted. As a result, CS can attract more hydroxyl groups onto the external of crosslinking network. On the other hand, in the crystallization area of PVA, water molecule is difficult to penetrate pure PVA membrane, because of the strong hydrogen bond existing in the chains of cross-linked PVA. Nevertheless, adding some CS into the PVA solutions could reduce the strength of hydrogen bond so that water molecules can pass through the membranes easily [26]. Fig. 4 also confirms that the swelling degree of the membrane decreases when the IPA content in the solution increases. The solution absorbed in the membrane increases with the increase of water content in solution, which results because membrane materials are highly hydrophilic.

### 6. Pervaporation Performance

#### 6-1. Effect of CS Content

Pervaporation-aided dehydration experiment of 90 wt% IPA solution at 60 °C was carried out to study the effect of CS content in the composite membranes on the separation performance. Fig. 6 shows the permeation flux and separation factor of membranes are influenced by CS content. The permeation flux increased gradually from 26 to 618  $\text{g}/(\text{m}^2 \cdot \text{h})$  with the increase of CS content, but the separation factor increased to the maximum value when the CS content was 60 wt% and then decreased significantly from 2140 to 16. The highest permeation flux 618  $\text{g}/(\text{m}^2 \cdot \text{h})$  but the lowest separation factor 16 were obtained for the CS/PVDF membrane because of the loose structure and big free volume of CS. When the CS/PVDF membrane was blended with PVA, the free volume of the crosslinking network in the matrix decreased. It resulted in a lower permeate flux. Also, the variation of the permeation flux was consistent with the membrane swelling extent.

#### 6-2. Effect of GA Content

The amount of crosslinking agent GA had a significant effect on membrane separation performance. The crosslinking agent triggers a chemical reaction between the polymers to enhance the swelling resistance of membranes in liquid. The membranes of CS content 60 wt% were selected to investigate the effect of the content of crosslinking agent on membrane separation performance under feed

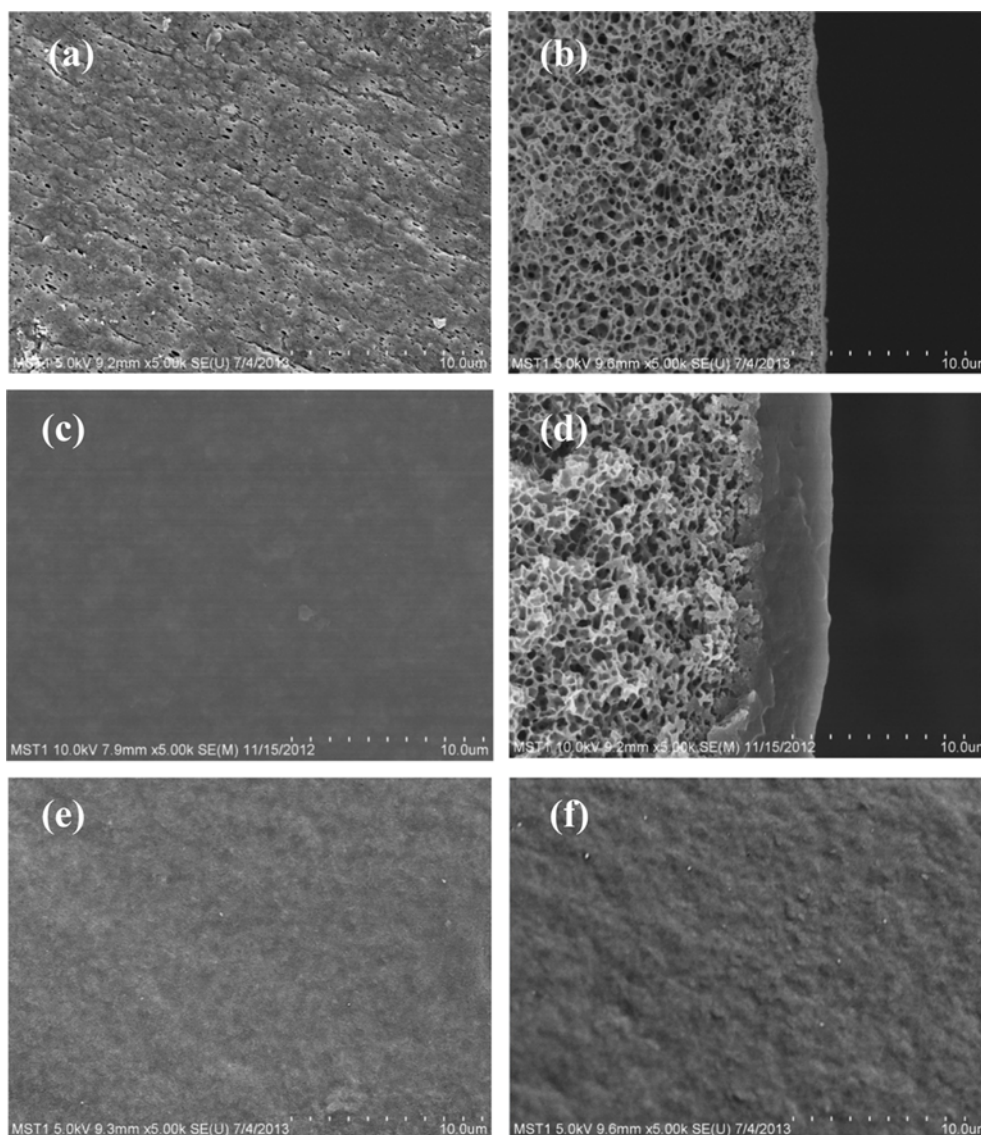


Fig. 4. SEM images of hollow fiber membranes: surface and cross-section images of PVDF support (a), (b); surface and cross-section images of M2 (c), (d); (e) surface image of M2-1; (f) surface image of M2-1.

Table 2. Water contact angles of membranes influenced by the composition of polymer and the content of GA

Membranes	M0	M1	M2	M3	M4	M2-1	M2-2
Contact angle (°)	67.2	82.4	76.6	72.1	66.9	74.3	85.7

temperature of 60 °C and IPA content of 90 wt%. As can be seen from Fig. 7(a) and (b), the permeation flux was the highest when the GA content was 0.15 wt%, whereas the separation factor was small. As the content of GA decreased to 0.10 wt%, the separation factor increased significantly to more than 2000, but the flux reduced to 306 g/(m<sup>2</sup>·h) at the beginning. When the content of GA was 0.05 wt%, the permeation flux increased to 358 g/(m<sup>2</sup>·h), but the separation factor decreased to 20. Thus, the content of GA 0.10 wt% was the suitable for the membrane preparation.

#### 6-3. Effect of Feed Concentration

Fig. 8 depicts the effect of feed water content on permeation

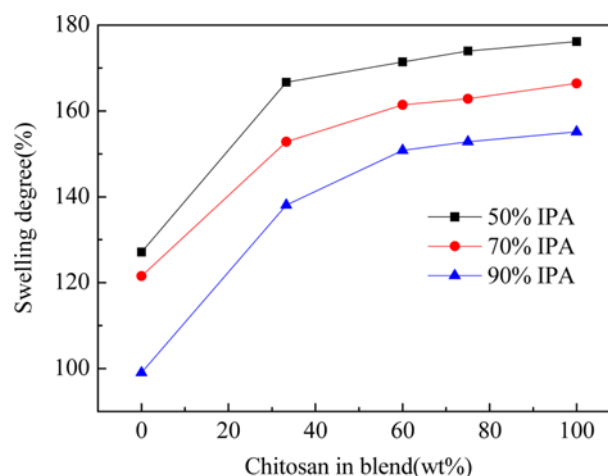


Fig. 5. Effect of IPA concentration in the mixture on the degree of swelling of membranes influenced by the ratio of polymer.



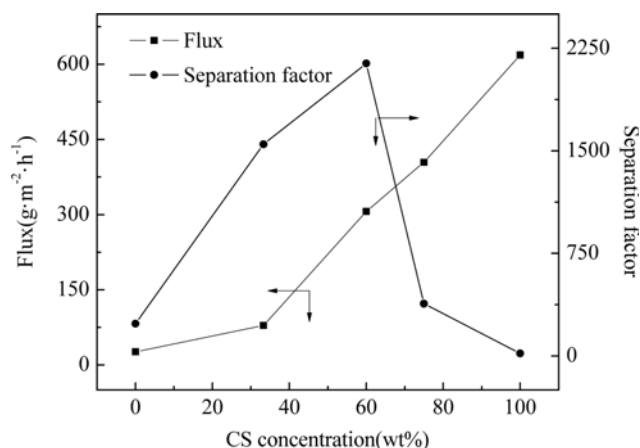


Fig. 6. Permeation flux and separation factor for dehydration of 90 wt% IPA solution against CS concentration in the blend membranes at 60 °C.

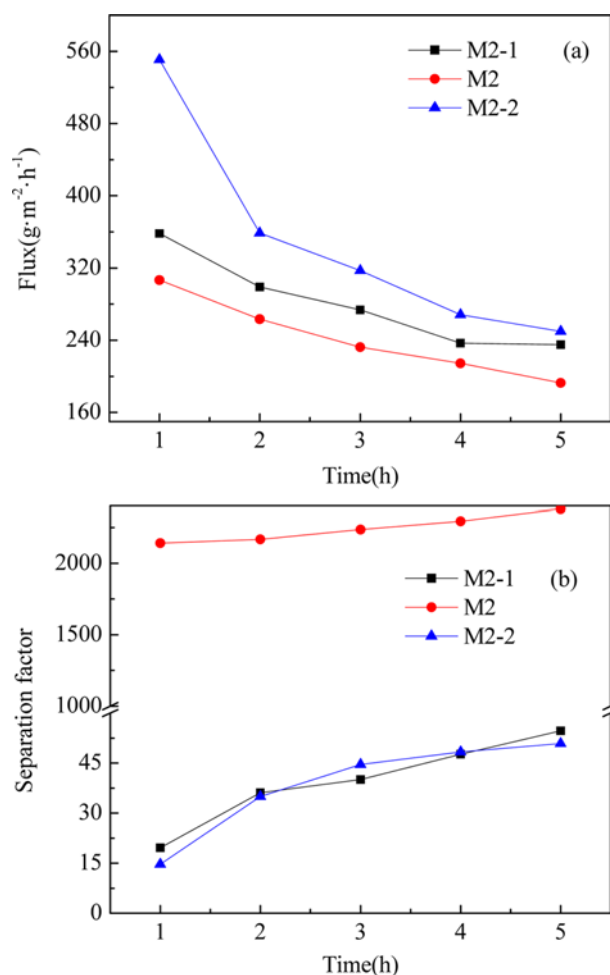


Fig. 7. Effect of GA content on permeation flux (a) and separation factor (b) of M2, M2-1 and M2-2 for dehydration of 90 wt% IPA solution at 60 °C.

flux and separation factor using M2. The experiment was investigated over a range of feed content from 3 wt% to 15 wt% at constant temperature of 60 °C. As can be seen from Fig. 7, the per-

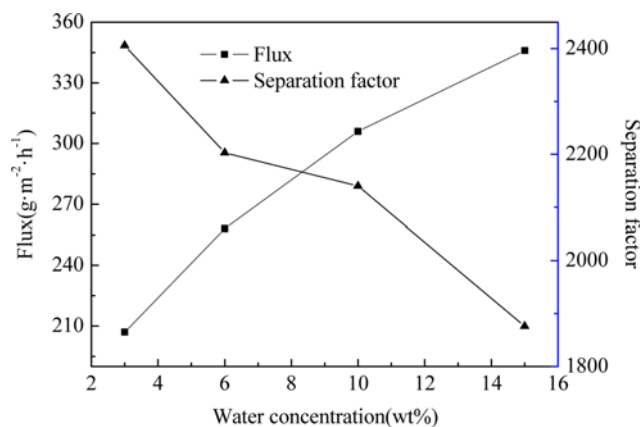


Fig. 8. Effect of feed concentration on permeation flux (a) and separation factor (b) of M2 for dehydration of IPA solution at 60 °C.

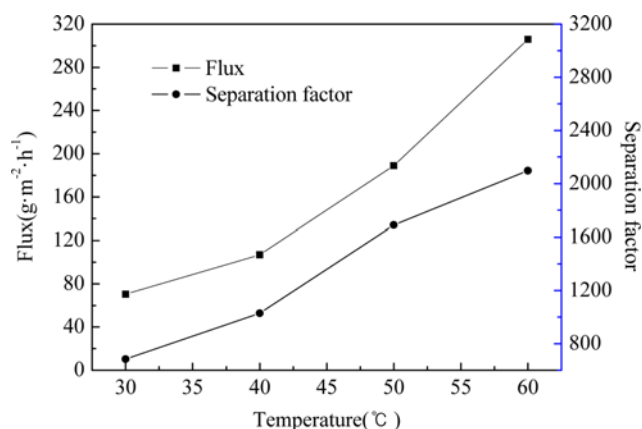


Fig. 9. Effect of feed temperature on permeation flux and separation factor of M2 for dehydration of 90 wt% IPA solution.

meation flux increased from 207 to 346  $\text{g}/(\text{m}^2 \cdot \text{h})$ , while the separation factor correspondingly decreased from 2406 to 1876. The higher content of water in the feed mixture led to the higher swelling capacity of the hydrophilic layer of membrane, so that a large number of water molecules and some IPA molecules could through the membrane more easily. As a consequence, the total permeation flux increased and the separation factor decreased with the increase of water content in the feed solution.

#### 6-4. Effect of Feed Temperature

The feed temperature is an important factor on membrane pervaporation performance. PV dehydration experiments were performed with 90 wt% IPA solution from 30 °C to 60 °C and the results are shown in Fig. 9. With the increasing temperature, the separation factor and permeation flux increased gradually. With the increase of temperature, the vapor pressure difference increased between the upstream and downstream side of the membranes, which resulted in the enhancement of the driving force of transport. Furthermore, the increasing temperature increased the diffusion rate of molecules. What's more, as the temperature increased, the thermal mobility and the free volume of polymer were elevated, which led to the increase of the solubility of solution on the surface. In

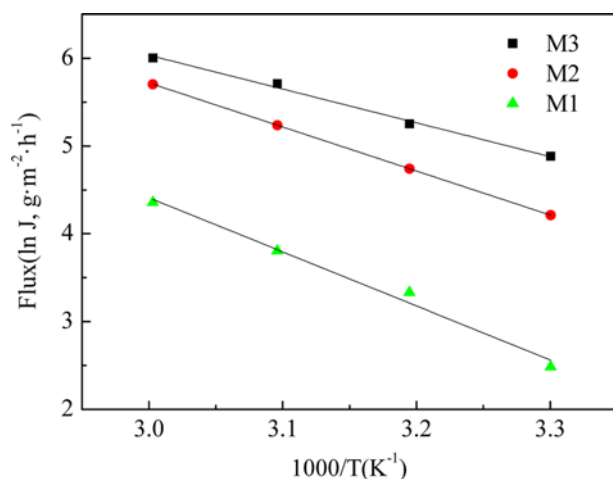


Fig. 10. Arrhenius relationship between permeation flux and feed temperature reciprocal of M1, M2 and M3 for pervaporation dehydration of 90 wt% IPA solution.

addition, the activation energy for permeation through the membrane can be described by Arrhenius relationship in Eq. (4):

$$J = J_0 \exp\left(\frac{-E_f}{RT}\right) \quad (4)$$

where  $J$  is the permeation flux,  $J_0$  is the pre-exponential factor,  $E_f$  refers to the activation energy for permeation,  $R$  and  $T$  are the gas constant and the absolute temperature, respectively. From Fig. 10, the activation energies for permeation flux of M1, M2 and M3 were calculated from the slope of the fit liners and the values were 32.0 kJ, 41.7 kJ and 51.2 kJ, respectively. The results indicated that increasing the content of CS could reduce the energy of molecules to penetrate through the membranes.

#### 6-5. Comparison with the Literature

Table 3 summarizes the flux and separation factor of different membranes for pervaporation dehydration of isopropanol. The separation performance of membrane CS:PVA (80:20) [12] is better

Table 3. Comparison of pervaporation performance for the dehydration of isopropanol with literatures

Membrane	Water content	T	Flux	Separation factor	References
CS/TDI	8.4	30	79	472	27
PVA-Fe(c)-4.5	10	30	79	470	28
PVA/Na <sup>+</sup> MMT-5	10	30	51	1116	29
CS/PVA(75:25)	10	60	644	-	4
CS-HPC-20	10	60	193	857	30
CS/PVA(80:20)	10	30	113	17991	12
CS-g-PANI	10	30	48	301	31
PVA/PVP-PMA	10	60	222	400	32
PVA-60	10	60	82	1492	33
PBI-CS	30	70	250	108	34
CS-PVA/PVDF	10	30	70	683	This study
CS-PVA/PVDF	10	60	306	2140	This study

than membranes reported by us. The reason is possibly that we used a different crosslinking agent. However, the permeation flux of membranes [27,28] is slightly higher than the CS-PVA/PVDF membrane, but the separation factor is less than the CS-PVA/PVDF membrane. When the feed temperature is 60 °C, the flux and separation factor of the developed membranes are higher than those membranes reported by the literature [30,32-34]. The developed CS-PVA/PVDF composite membrane using PVDF hollow fiber as support is a new and effective PV membrane for dehydration of isopropanol. It could be a prospective commercial membrane for dehydration of solvents.

## CONCLUSIONS

The composite membrane CS-PVA/PVDF was prepared on a PVDF hollow fiber support for pervaporation dehydration of IPA aqueous solution. Effects of the ratio of CS:PVA in casting solutions and the concentration of GA were investigated. ATR-FTIR confirmed the GA had crosslinked the blend membranes. The SEM images showed that dense separation layers were successfully coated onto the supports. TG measurement showed that the stability of membrane with CS content 60 wt% was better than the others. With the increase of CS content in the polymer, the water contact angle increased. The swelling degree of membrane increased with the increase of CS concentration. When the CS and GA content were 60 wt% and 0.10 wt%, respectively, the permeate flux was 306 g/(m<sup>2</sup>·h) with water content of nearly 100% in the permeate for a feed solution containing 90 wt% isopropanol at 60 °C. The permeation flux increased with the increasing feed water concentration, while the separation factor decreased. The separation factor and permeation flux increased with the increasing feed temperature. Comparing the results with the literature, the new hollow fiber composite membranes prepared in this work could be a good candidate for industrial PV dehydration of IPA solutions.

## ACKNOWLEDGEMENTS

This work was financially supported by National Key Science and Technology Program of China (No.2013BAE11B01) and Jiangsu Province Natural Science Foundation for University of China (No. 11KJB530005).

## REFERENCES

1. P.D. Chapman, T. Oliveira, A. G. Livingston and K. Li, *J. Membr. Sci.*, **318**, 5 (2008).
2. S. B. Kuila and S. K. Ray, *Sep. Purif. Technol.*, **89**, 39 (2012).
3. A. M. Sajjan, B. K. Jeevan Kumar, A. A. Kittur and M. Y. Karidurganavar, *J. Ind. Eng. Chem.*, **19**, 427 (2013).
4. A. Svang-Ariyaskul, R. Y. M. Huang, P. L. Douglas, R. Pal, X. Feng, P. Chen and L. Liu, *J. Membr. Sci.*, **280**, 815 (2006).
5. D. P. Suhas, T. M. Aminabhavi and A. V. Raghu, *Polym. Eng. Sci.*, **54**, 1774 (2014).
6. D. P. Suhas, A. V. Raghu, H. M. Jeong and T. M. Aminabhavi, *Rsc. Adv.*, **3**, 17120 (2013).
7. S. G. Adoor, V. Rajinekanth, M. N. Nadagouda, K. Chowdoji Rao,

- D. D. Dionysiou and T. M. Aminabhavi, *Sep. Purif. Technol.*, **64**, 113 (2013).
8. J. M. Yang and H. C. Chiu, *J. Membr. Sci.*, **419**, 65 (2012).
9. P. Y. Zhuang, Y. L. Li, L. Fan, J. Lin and Q. L. Hu, *Int. J. Biol. Macromol.*, **50**, 658 (2012).
10. M. Ionita and H. Iovu, *Composites Part B*, **43**, 2464 (2012).
11. M. N. Hyder and P. Chen, *J. Membr. Sci.*, **340**, 171 (2009).
12. K. Rao, M. C. S. Subha, M. Sairam, N. N. Mallikarjuna and T. M. Aminabhavi, *J. Appl. Polym. Sci.*, **103**, 1918 (2007).
13. V. T. Magalad, A. R. Supale, S. P. Maradur, G. S. Gokavi and T. M. Aminabhavi, *Chem. Eng. J.*, **159**, 75 (2010).
14. V. T. Magalad, G. S. Gokavi, K. V. S. N. Raju and T. M. Aminabhavi, *J. Membr. Sci.*, **354**, 150 (2010).
15. V. T. Magalad, G. S. Gokavi, C. Ranganathaiah, M. H. Burshe, C. Han, D. D. Dionysiou, M. N. Nadagouda and T. M. Aminabhavi, *J. Membr. Sci.*, **430**, 321 (2013).
16. V. T. Magalad, G. S. Gokavi, M. N. Nadagouda and T. M. Aminabhavi, *J. Phys. Chem. C*, **115**, 14731 (2011).
17. R. X. Liu, X. Y. Qiao and T. S. Chung, *J. Membr. Sci.*, **294**, 103 (2007).
18. H. K. Yuan, J. Ren, X. H. Ma and Z. L. Xu, *Desalination*, **280**, 252 (2011).
19. C. J. Liao, P. Yu, J. Q. Zhao, L. M. Wang and Y. B. Luo, *Desalination*, **272**, 59 (2011).
20. Z. G. Zhao, J. F. Zheng, M. J. Wang, H. Y. Zhang and C. C. Han, *J. Membr. Sci.*, **394**, 209 (2012).
21. P. Sukitpaneenit and T. S. Chung, *J. Membr. Sci.*, **374**, 67 (2011).
22. P. Sukitpaneenit, T. S. Chung and L. Y. Jiang, *J. Membr. Sci.*, **362**, 393 (2011).
23. E. Salehi, S. S. Madaeni, L. Rajabi, V. Vatanpour, A. A. Derakhshan, S. Zinadini, S. Ghorabi and H. Ahmadi Monfared, *Sep. Purif. Technol.*, **89**, 309 (2012).
24. J. Li and B. Renbi, *Langmuir*, **18**, 9765 (2002).
25. S. Meenakshi, S. D. Bhat, A. K. Sahu, P. Sridhar, S. Pitchumani and A. K. Shukla, *J. Appl. Polym. Sci.*, **124**, E73 (2012).
26. Q. Yu, Y. Song, X. Shi, C. Xu and Y. Bin, *Carbohydr. Polym.*, **84**, 465 (2011).
27. D. Anjali Devi, B. Smitha, S. Sridhar and T. M. Aminabhavi, *J. Membr. Sci.*, **262**, 91 (2005).
28. M. Sairam, B. V. K. Naidu, S. K. Nataraj, B. Sreedhar and T. M. Aminabhavi, *J. Membr. Sci.*, **283**, 65 (2006).
29. S. G. Adoor, M. Sairam, L. S. Manjeshwar, K. V. S. N. Raju and T. M. Aminabhavi, *J. Membr. Sci.*, **285**, 182 (2006).
30. R. S. Veerapur, K. B. Gudasi and T. M. Aminabhavi, *J. Membr. Sci.*, **304**, 102 (2007).
31. J. G. Varghese, A. A. Kittur, P. S. Rachipudi and M. Y. Kariduragannavar, *J. Membr. Sci.*, **364**, 111 (2010).
32. M. G. Mali, V. T. Magalad, G. S. Gokavi, T. M. Aminabhavi and K. V. S. N. Raju, *J. Appl. Polym. Sci.*, **121**, 711 (2011).
33. M. Heydari, A. Moheb, M. Ghiaci and M. Masoomi, *J. Appl. Polym. Sci.*, **128**, 1640 (2013).
34. Y. J. Han, K. H. Wang, J. Y. Lai and Y. L. Liu, *J. Membr. Sci.*, **463**, 17 (2014).